

Resilience of Electricity Distribution Networks - Part I: Cyber-physical Disruption Models

Devendra Shelar, Saurabh Amin, and Ian Hiskens

Abstract—This work contributes to the need for developing a systematic approach to evaluate and improve the resilience of electricity distribution networks (DNs) to cyber-physical failure events. We introduce a failure model that captures the joint impact of physical failures that result in the transmission network as voltage disturbances and cyberattacks to DN components that cause supply-demand disturbances at multiple nodes. The model is used to formulate a bilevel mixed-integer problem that captures the sequential interaction between an attacker (leader) and the DN operator (follower). The attacker (resp. operator) aims to maximize (resp. minimize) the post-contingency loss resulting from the cyber-physical failure events. We solve this problem by applying the Benders Decomposition algorithm to an equivalent min-cardinality disruption problem. Our solution approach relies on a reformulation of the “coupling constraints” which model the effects of the attacker’s discrete actions on the set of feasible operator response strategies. We evaluate the operator’s value of timely response as the net reduction in post-contingency loss compared to the case with no response. This reduction can be viewed as the improvement in DN resiliency against the class of cyber-physical failure events.

Index Terms—Cyber-physical systems, network security, smart grids, bilevel optimization

I. INTRODUCTION

Despite the recent trends in modernization of electricity Distribution Networks (DNs), many Distribution System Operators (DSOs) continue to face both strategic and operational challenges in ensuring a reliable and secure service to their customers. On one hand, the integration of new supply sources such as Distributed Generators (DGs) and new monitoring and control capabilities enable flexible DN operations [1, 2, 3, 4]. On the other hand, these capabilities also expose the inherent vulnerabilities of DN components to remote adversaries [5, 6, 7, 8], which may include criminal organizations, terrorist groups, and nation states.

Security threats to DNs can escalate in the presence of intermittent disturbances in the Transmission Network (TN), or during conditions when the power system is close to an emergency state [9, 10, 11]. It is well-recognized that successful cyber-physical failures in TN/DN – individually or in combination – can result in

to a significant disruption in the system operation, and lead to contingencies such as violations in the operating bounds of system state and/or loss in the functionality of network components. This paper is motivated by the DSO’s need for responding to such contingencies in a timely manner to prevent (or at least delay) the automatic protection mechanisms from triggering and causing extensive uncontrolled load/DG disconnects (outage). The main hypothesis is that the operational flexibility of modern DNs can be exploited to generate a timely response to cyber-physical failures (particularly security attacks). We show that such a response can lead to significant reduction in the post-contingency losses. This capability becomes especially important for DNs facing risk of correlated failures under which the traditional undervoltage protection mechanisms may no longer be adequate or not trigger at all.

More broadly, we contribute to a framework for evaluating DN resilience. As such, resilience of a system is defined as “its ability to prepare and plan for, absorb, recover from, and more successfully adapt to adverse event” [12]. Indeed, previous literature has dealt with issues related to resiliency of power systems [6, 10, 11]. However, these approaches do not explicitly model the combined effects of TN- and DN-side failure scenarios on the losses faced by the DSO, and cannot be directly used to evaluate the effectiveness of available response strategies. We develop a simple yet generic approach to address this gap in the literature.

We say that a DN with an operational response capability is *more resilient* to a class of cyber-physical failures if the DSO incurs a *lesser* post-contingency loss when subjected to these failures, relative to the loss under “no response” or classical protection mechanisms. Indeed, defining a relevant class of failure scenarios, DSO response strategy, and acceptable extent of post-contingency loss are all important aspects of the problem. Also important is a computationally tractable approach to evaluate “worst-case” post-contingency loss. To address these aspects, we first introduce an attack model to capture DN-side failure scenarios that are relevant to cyberphysical security of DNs [5]. We argue that the impact of such security failures may aggravate under TN-side reliability failures. The effect of TN-side failure is modeled as a voltage sag (drop in the substation voltage), while the DN-side failures are modeled as supply-demand disturbances at the DN nodes. For the sake of concreteness, we consider a remote attack on the DG

Manuscript submitted on December 7, 2018. This work was supported by NSF project “FORCES” (award #: CNS-1239054).

D. Shelar and S. Amin are with Department of CEE, at MIT (shelard,amins@mit.edu, phone: 857-253-8964). I. Hiskens is with Department of EECS at UMich (hiskens@umich.edu).

Management System (DGMS) server that can lead to sudden and simultaneous disruptions of multiple DGs in the DN.

Next, we consider the response capabilities supported by modern DNs. Broadly speaking, these capabilities can be classified as follows: (a) Remote control by the DSO/control center during nominal operating conditions; for example, load control and control of DGs (through DGMS); (b) autonomous disconnect operation of individual components based on local information; for example, tripping of DGs or loads under nodal violations in operating conditions; and (c) emergency control at the substation level which is typically executed by the Substation Automation (SA) system. Please refer to Fig. 1 for an illustration. For a review of the current and future DN control capabilities, the reader is referred to [13].

Since our security attack model considers the compromise of remote control capabilities of the DGMS, (a) is no longer a viable response mechanism. However, (b) or (c) can be still viewed as a plausible response to the attack-induced disturbance.

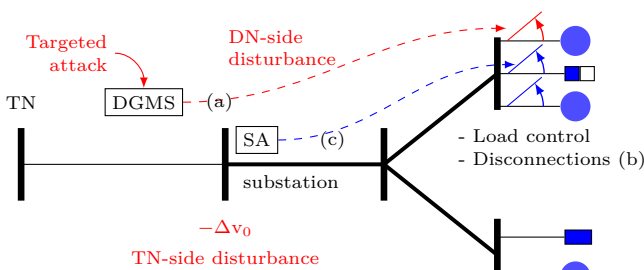


Fig. 1: Attacker-operator interaction.

Next, we present a computational approach to solve a bilevel optimization problem for evaluating the maximum post-contingency loss when the DSO optimally responds to the attack. In particular, in this formulation, the DSO response comprises of load control and preemptive tripping of components (loads and/or DGs). The DSO can operationalize such a timely response via the SA systems, which were recently provided cyber-security perimeter by the NERC regulations [14]. In comparison, the new control center operations such as DGMS are prone to back channel attacks by remote third parties, as evident from the recent incidents [15]. By evaluating the reduction in loss due to a timely DSO response, and comparing it with the loss under the no response action, we can estimate the *value* of the timely response strategy toward the DN's resilience.

Our bilevel formulation models the sequential interaction between a strategic attacker and the operator; see [4, 9, 16, 17] for similar formulations. The formulation can be stated as follows:

$$\mathcal{L}_{\text{Mm}} := \max_{d \in \mathcal{D}} \min_{u \in \mathcal{U}(d)} L(u, x) \quad \text{s.t.} \quad x \in \mathcal{X}(u), \quad (\text{P1})$$

where x denotes the post-contingency network state, i.e. the state after the attacker-operator interaction is completed; \mathcal{X} denotes the set of constraints that model physical constraints (power flows), component constraints (loads and DGs), and nodal voltage constraints (Sec. II); d denotes an attacker-induced failure; u denotes an operator response; \mathcal{D} denotes the set of attacker's strategies (Sec. III); $\mathcal{U}(d)$ denotes the *coupling* constraints that model the impact of attack-induced failures on the set of feasible operator responses (Sec. IV). For a given disruption $d \in \mathcal{D}$, the operator's objective is to minimize the post-contingency loss $L(u, x)$. And the attacker's objective is to choose an attack that maximizes the post-contingency loss assuming an optimal response by the operator. Suppose that (d^*, u^*) is an optimal solution to this maximin problem which results in the network state x^* . Then $\mathcal{L}_{\text{Mm}} = L(u^*, x^*)$ is the post-contingency loss that operator will incur when he implements u^* in response to the attack d^* (Sec. V-A).

Essentially, problem (P1) is a Bilevel Mixed Integer Problem (BiMIP) formulation. In principle, the Benders Decomposition (BD) algorithm can be applied to solve such formulations. However, in our problem only integer variables enter in the coupling constraints. It turns out in such cases, a straightforward application of BD algorithm does not generate useful Benders cuts. Our solution approach addresses this issue by formulating an equivalent min-cardinality disruption problem and reformulating the coupling constraints to ensure that the set of attack vectors are progressively refined in each iteration of BD algorithm (Sec. V-B).

The post-contingency loss \mathcal{L}_{Mm} is a measure of the maximum reduction in system performance under the class of disruptions in the set \mathcal{D} ; see Fig. 2. For the sake of normalization, we denote by \mathcal{L}_{max} the loss incurred by operator when all loads and DGs are disconnected. Then, $\mathcal{R}_{\text{Mm}} := 100 \left(1 - \frac{\mathcal{L}_{\text{Mm}}}{\mathcal{L}_{\text{max}}}\right)$ can be viewed as the resilience metric of the DN.

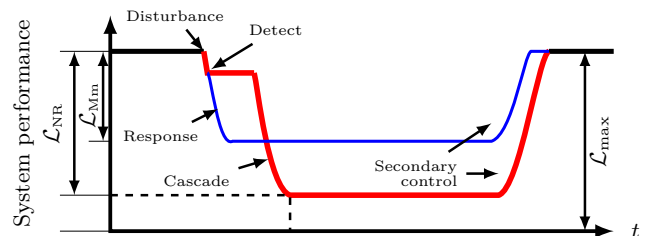


Fig. 2: System performance with and without operator response.

Now suppose that we want to compare the DN resilience under operator response to the case of no response. To do this comparison, we need to find the maximum loss corresponding to automatic disconnects of DN components that would be induced by an attack d_{nr}^* , i.e. uncontrolled cascade-like loss in load/DG connectivity due to operating voltage bound violations (Algorithm 1).

Let the automatic disconnect actions be denoted by u_{nr} , resulting network state by x_{nr} , and the corresponding loss by $\mathcal{L}_{NR} = \mathcal{L}(x_{nr}, u_{nr})$. Then, the resilience metric of the DN under no response can be written as $\mathcal{R}_{NR} = 100(1 - \mathcal{L}_{NR}/\mathcal{L}_{max})$. Naturally, $\mathcal{R}_{Mm} \geq \mathcal{R}_{NR}$, and we can evaluate the relative value of operational response (or equivalently, the improvement in DN resilience) as $(\mathcal{R}_{Mm} - \mathcal{R}_{NR})$. In Sec. V-C, we evaluate this quantity for a set of test DNs.

II. NETWORK MODEL

DN parameters

\mathcal{N}	set of nodes in DN
\mathcal{E}	set of edges in DN
0	substation node label
\mathcal{G}	radial topology of DN $\mathcal{G} = (\mathcal{N} \cup \{0\}, \mathcal{E})$
$N = \mathcal{N} $	number of non-substation nodes in DN
\mathbf{j}	complex square root of -1, $\mathbf{j} = \sqrt{-1}$
v^{nom}	nominal squared voltage magnitude (1 pu)
v_0	squared voltage magnitude at substation node

Nodal quantities of node $i \in \mathcal{N}$

v_i	squared voltage magnitude at node i
$\overline{pc}_i + \mathbf{j}\overline{qc}_i$	nominal demand at node i
$\overline{pg}_i + \mathbf{j}\overline{qg}_i$	nominal generation at node i
$pc_i + \mathbf{j}qc_i$	actual power consumed at node i
$pg_i + \mathbf{j}qg_i$	actual power generated at node i
$p_i + \mathbf{j}q_i$	net power consumed at node i
$\underline{vc}_i, \overline{vc}_i$	lower, upper voltage bounds for load i
$\underline{vg}_i, \overline{vg}_i$	lower, upper voltage bounds for DG i
kg_i	0 if DG i is connected to DN; 1 otherwise
kc_i	0 if load i is connected to DN; 1 otherwise
β_i	fraction of demand satisfied at node i
$\underline{\beta}_i$	lower bound of load control parameter β_i

Parameters of edge $(i, j) \in \mathcal{E}$

$P_{ij} + \mathbf{j}Q_{ij}$	power flowing from node i to node j
$\mathbf{r}_{ij}, \mathbf{x}_{ij}$	resistance and reactance of line $(i, j) \in \mathcal{E}$

Attack variables

$d \in \{0, 1\}^{\mathcal{N}}$	$d_i = 1$ if DG i is disrupted; 0 otherwise.
--------------------------------	--

Operator response variables

u	an operator response action
-----	-----------------------------

TABLE I: Table of Notations.

Since more than 95% of DNs have radial topologies, we model DN as a tree network of node set $\mathcal{N} \cup \{0\}$ and line set \mathcal{E} ; see Fig. 3. We refer the reader to Table I for the definitions of key notations, and to references [3, 8] for further details.

For the sake of computational simplicity, we model the power flows using the classical *LinDistFlow* model [18]:

$$P_{ij} = \sum_{k:(j,k) \in \mathcal{E}} P_{jk} + p_j \quad \forall (i, j) \in \mathcal{E} \quad (1)$$

$$Q_{ij} = \sum_{k:(j,k) \in \mathcal{E}} Q_{jk} + q_j \quad \forall (i, j) \in \mathcal{E} \quad (2)$$

$$v_j = v_i - 2(\mathbf{r}_{ij}P_{ij} + \mathbf{x}_{ij}Q_{ij}) \quad \forall (i, j) \in \mathcal{E}, \quad (3)$$

where (1)-(2) are the power conservation equations and (3) is the voltage drop equation.

Without loss of generality, we assume that each node of the DN has a load and a DG. Furthermore, we consider the constant power model for both loads and DGs.

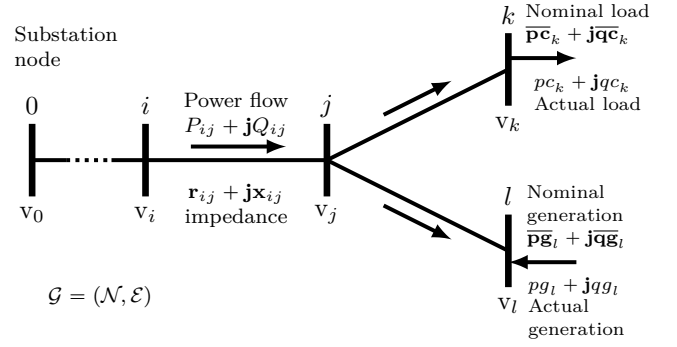


Fig. 3: DN model.

DG model: Depending on whether a DG is connected to the network or not, its actual output is related to its nominal output as follows:

$$pg_i = (1 - kg_i) \overline{pg}_i, \quad qg_i = (1 - kg_i) \overline{qg}_i. \quad (4)$$

According to the IEEE standard rules for interconnection of DGs [19], to ensure safety as well as proper functioning of the components, DGs are required to disconnect from the DN if voltage bound violations occur. We model this constraint as follows:

$$kg_i \geq \underline{vg}_i - v_i, \quad kg_i \geq v_i - \overline{vg}_i \quad \forall i \in \mathcal{N}. \quad (5)$$

Load model: In many smart DNs, the operator can change its actual consumption of a connected load to a fraction of its nominal demand via direct load control in response to supply-demand disturbance [2]. We model this flexibility as the choice of load control parameter $\beta_i \in [\underline{\beta}_i, 1]$, i.e. when $kc_i = 0$, and $\beta_i = 0$ when $kc_i = 1$. Here $\underline{\beta}_i \in [0, 1]$ denotes the minimum fraction of the load's nominal demand that should be satisfied provided the load is connected. This load control capability can be represented as the mixed-integer linear constraints:

$$pc_i = \beta_i \overline{pc}_i, \quad qc_i = \beta_i \overline{qc}_i \quad \forall i \in \mathcal{N}, \quad (6)$$

where

$$(1 - kc_i) \underline{\beta}_i \leq \beta_i \leq (1 - kc_i) \quad \forall i \in \mathcal{N}. \quad (7)$$

Similar to DGs, the connectivity of loads also depends on the nodal voltages which can be modeled as follows:

$$kc_i \geq \underline{vc}_i - v_i, \quad kc_i \geq v_i - \overline{vc}_i \quad \forall i \in \mathcal{N}. \quad (8)$$

Then, the net actual consumption at nodes is given by:

$$p_i = pc_i - pg_i, \quad q_i = qc_i - qg_i \quad \forall i \in \mathcal{N}. \quad (9)$$

We define the network state $x \in \mathbb{R}^{5N}$ as $x := (p, q, P, Q, v)$, where p, q, P, Q, v are row vectors of appropriate dimensions.

III. CYBER-PHYSICAL FAILURE MODEL

Now, we describe a generic cyber-physical failure model that captures the effects of DN-side component disruptions caused by security failures as well as effects of disturbances from the TN.

DN-side disruption: Our attack model is motivated by the security failure scenarios listed in [5]. For the sake of concreteness, we consider a specific attack scenario in which the attacker targets the DGMS server, with the aim to simultaneously disrupt multiple DGs connected to the DN. Our modeling approach can also accommodate other important attack scenarios such as mass remote disconnects of loads or invalid load control commands [5], as shown in our previous work [4].

Let $d \in \{0, 1\}^{\mathcal{N}}$ be a vector denoting the disrupted nodes, where $d_i = 1$ if node i is disrupted, otherwise $d_i = 0$. Let k be the maximum number of nodes that the attacker can disrupt (i.e. resource constraint), and let $\mathcal{D} := \{d \in \{0, 1\}^{\mathcal{N}} \mid \sum_{i \in \mathcal{N}} d_i \leq k\}$ denote the set of feasible attacker strategies. This constraint limits the attacker’s ability to disrupt arbitrary number of nodes. For the purpose of evaluating DN’s resilience to security attacks, one can consider that the existing fail-safe mechanisms employed by the operator (including the in-built “hard” security checks within the DGMS software) do not permit simultaneous disruptions of DG nodes beyond a certain limit. This limit can be taken as the choice of k .

Our attack model assumes that by compromising the DGMS, the attacker can access information needed to strategically choose the disruption vector d . This includes DN topology, line resistances and reactances, nominal nodal demands and DG outputs, and the value of substation voltage deviation due to TN-side disturbance. Note that this data is already collected by the DGMS to control DG output (e.g. for Volt-VAr regulation). Thus, one can assume that the attacker can also access it.

Furthermore, our attacker model considers that the DGMS (which is typically hosted by the control center) is a more viable target for remote external attackers than local substation automation (SA) systems. Indeed, recent incidents [15] have indicated that control center/DGMS servers can be targets of sophisticated phishing attacks (for e.g. through a download of infected email attachments by the human operators who manage these servers). In contrast, a growing number of distribution utilities are regulated under NERC CIP standards which secure the substations against remote attacks via reperimetrization of the substation cyber architecture [14, 20]. In addition, SA is typically not prone to insecure actions by human insiders. As recent incidents [15] indicate, control center/DGMS servers can be targets of sophisticated phishing attacks (for e.g. through a download of infected email attachments by the human operators who manage these servers.)

Now we model the impact of attacker’s actions on the DN state. If the attacker disrupts a DG at node i , then that DG becomes non-operational, and is *effectively disconnected* from the DN, i.e

$$kg_i \geq d_i \quad \forall \quad i \in \mathcal{N}. \quad (10)$$

The disconnections of DGs lead to a sudden drop in reactive power supply. Under heavy loading (high

demand) conditions, reactive power cannot be supplied immediately from the bulk supply sources through the transmission lines. The reactive power shortfall can further worsen in the presence of voltage dip resulting from a TN-side disturbance (see below). This may result in sustained low-voltage conditions, for e.g. a Fault-induced delayed voltage recovery (FIDVR) event [21, 22]. Our operator model (Sec. IV) uses SA to implement an operational response to attack-induced disruptions.

TN-side disturbance: Our model of TN-side disturbance is motivated by situations such as failure of a transmission line or a bulk generator, in which FIDVR lasts for a prolonged period (several minutes). We model its impact as a sudden drop in the substation node’s voltage by Δv_0 , which we assume to be exogenously given (and fixed). Thus, the substation voltage in the presence of a TN-side disturbance can be written as follows:

$$v_0 = v^{\text{nom}} - \Delta v_0. \quad (11)$$

Indeed, $\Delta v_0 = 0$ indicates no TN-side disturbance. Since our focus is on DN-side disruptions, we consider the TN-side disturbance parameter as an exogenously given (fixed) parameter of the problem.

Note that TN-side disturbance can also result in a change in frequency away from the nominal operating frequency of the network. We extend our model to include frequency disturbances in the companion paper [23]. Finally, we emphasize that the impact of attack-induced disruptions on DN can be quite severe when the DN is simultaneously facing such TN-side disturbance. For instance, the attacker can program the DN-side attack to be launched only when substation voltage reading drops at least by Δv_0 .

IV. OPERATOR MODEL

Recall that two operator response mechanisms that we consider are the autonomous disconnect operations and emergency control by the substation automation; see Fig. 1. Now, we describe these mechanisms in detail.

A. Autonomous Component Disconnections

The autonomous disconnect operation is based on local checks of operating bounds at the DN nodes. This is typically the case for legacy DN management systems where the operator does not have access to node-level data. Consequently, an operator relying solely on this mechanism does not have the ability to timely detect, accurately identify, and promptly respond to coordinated supply-demand disturbances in the DN, which is indeed the case in our attack model. As such, one can view this mechanism simply as “no response” from the operator, since the disconnect operations are local and do not need network-level coordination by the operator. Henceforth we adopt the term “no response” to represent (b).

To model the network state under no response mechanism, we adopt and refine the *cascade algorithm* used in [24], which is well-suited for modeling forced tripping of

network components under operating bound violations. Specifically, [Algorithm 1](#) takes the initial network state at the start of attack-induced contingency (denoted x_{nr}), and generates automatic disconnect actions for one or more components, as the state evolves over multiple rounds of an uncontrolled cascade. Let the vector of variables representing the automatic disconnect actions be denoted by $u_{nr} = (\beta^{nr}, kc^{nr}, kg^{nr})$. In each round of the cascade, u_{nr} is updated based on disconnect actions on the components that violate the voltage bounds in that round. These actions are determined by checking [Equations \(5\) and \(8\)](#). Then, new power flows are computed after each round of disconnection by recomputing x_{nr} . Note that the load control parameter $\beta_i^{nr} = 1$ throughout the cascade, until the load gets fully disconnected. Since at least one component disconnect happens in each round, the algorithm terminates in at most $2N$ rounds. The final connectivity vector u_{nr} corresponds to a situation where all the connected components satisfy voltage bounds, and can be used to compute the post-contingency state and the corresponding loss.

Algorithm 1 Uncontrolled cascade under no response

- 1: Initialize $u_{nr} = (\beta^{nr}, kc^{nr}, kg^{nr}) = (\mathbf{1}, \mathbf{0}, d)$
 - 2: Compute state vector x_{nr} using [\(1\)-\(4\)](#), [\(6\)](#), [\(7\)](#), and [\(9\)](#)
 - 3: **while** $\exists i$ such that [\(5\)](#) is violated **do**
 - 4: set $kg_i^{nr} = 1$, update u_{nr}
 - 5: recompute x_{nr} using [\(1\)-\(4\)](#), [\(6\)](#), [\(7\)](#), and [\(9\)](#)
 - 6: **end while**
 - 7: **while** $\exists i$ such that [\(8\)](#) is violated **do**
 - 8: set $\beta_i^{nr} = 0, kc_i^{nr} = 1$, update u_{nr} , recompute x_{nr}
 - 9: **end while**
 - 10: **return** u_{nr}, x_{nr}
-

B. Emergency Response by System Automation

The emergency response mechanism exploits the capabilities of modern SA systems that have the visibility of node-level consumption, distributed generation, and nodal voltages. Many of the newer installations of Advanced Metering Infrastructures (AMIs) are already equipped with data logging and communication capabilities. If the AMIs are installed at medium-to-low-voltage transformers, these sensors can provide the SA with the node level data in real-time (every second). With this capability, sudden changes in local DG output can also be detected by the SA, thereby enabling the operator to identify the attack vector d .

To model the operator response through SA, we consider node-level data is used to determine the extent of load control (β) and intentional disconnects (kc, kg), and that this response is exercised through the substation automation. Let the set of allowable load control vectors be defined as $\mathcal{B} := \prod_{i \in \mathcal{N}} (\{0\} \cup [\beta_i, 1])$. Then, we can denote an operator response strategy as $u = (\beta, kc, kg) \in \mathcal{U}$, where $\mathcal{U} := \mathcal{B} \times \{0, 1\}^{\mathcal{N}} \times \{0, 1\}^{\mathcal{N}}$. Finally, we can denote the set of response strategies feasible after an attack d by $\mathcal{U}(d) := \{u \in \mathcal{U} \mid \text{such that (10) hold}\}$.

C. Post-contingency loss

Let L denote the post-contingency loss incurred by the operator. We define it as the sum of following costs: (i) cost due to loss of voltage regulation, (ii) cost of load control, and (iii) cost of load shedding:

$$L(u, x) = W_{VR} \|v^{\text{nom}} - v\|_{\infty} + W_{LC} \sum_{i \in \mathcal{N}} (1 - \beta_i) \overline{pc}_i + (W_{LS} - W_{LC}) \sum_{i \in \mathcal{N}} kc_i \overline{pc}_i, \quad (12)$$

where $W_{LC} \in \mathbb{R}_+$ denotes the cost of per unit load controlled, $W_{LS} \in \mathbb{R}_+$ and $W_{LS} \geq W_{LC}$ is the cost in dollars of per unit load shed, and $W_{VR} \in \mathbb{R}_+$ is the cost of unit absolute deviation of nodal voltage from the nominal value $v^{\text{nom}} = 1$ pu. [Table III](#) provides relative values of these costs.

We say that if no components are disconnected after the attacker-operator interaction, the DN is in the *No-Disconnect* (ND) regime; otherwise, it's in the *Component-Disconnected* (CD) regime. In the CD regime, the operator incurs an additional cost than the ND regime in form of compensation to the consumers whose loads are completely disconnected. Note that, in our model, the CD regime can result from an uncontrolled cascade under no response, or from emergency response by the SA system.

V. BILEVEL OPTIMIZATION PROBLEM

A. Formulation

Let \mathcal{X} denote the set of post-contingency states x that satisfy the constraints [\(1\)-\(9\)](#). Now, we can model the attacker-operator interaction as a sequential game:

$$\begin{aligned} \mathcal{L}_{\text{Mm}} := & \max_{d \in \mathcal{D}} \min_{u \in \mathcal{U}(d)} L(u, x) \\ & \text{s.t. } x \in \mathcal{X}(u), \end{aligned} \quad (\text{Mm})$$

Thus, the attacker's (resp. operator's) objective is to maximize (resp. minimize) the loss L subject to [LinDistFlow \(1\)-\(3\)](#), DG and load models [\(4\)-\(9\)](#), and failure impact models $u \in \mathcal{U}(d)$ and [\(11\)](#). Following [\[9\]](#), we refer the problem [\(Mm\)](#) as the *Budget-k-max-loss* problem [\[9\]](#), where k is the budget of the attacker, and determines \mathcal{D} . It is easy to see that [\(Mm\)](#) is a bilevel mixed-integer program (BiMIP).

In the no response case, for a given attacker action d , [Algorithm 1](#) allows us to compute the final state of operator variables u_{nr} and network state x_{nr} . We can then evaluate the post-contingency loss $L(u_{nr}, x_{nr})$ for an attack-induced DG disruption vector $d \in \mathcal{D}$ in the no response case by using [Equation \(12\)](#). For any given attack cardinality k , we denote the maximum over no-response post-contingency losses of all attack vectors by \mathcal{L}_{NR} . The optimal attack vector can be computed by simple enumeration over attacks of cardinality k .

B. Solution Approach

To evaluate the post-contingency loss in the case of emergency response by the SA, we need to solve the bilevel problem [\(Mm\)](#), which has both integer variables

in both inner and outer problems. In general, such BiMIP problems are NP-hard and are computationally challenging to solve [16, 24]. Our solution approach relies on using the Benders Decomposition (BD) algorithm to approximately solve (Mm) on a reformulated problem. The overall approach can be described as follows. First, we argue that \mathcal{L}_{Mm} can be obtained by solving an equivalent *Min-cardinality disruption* problem instead. Then, we apply the BD algorithm, which decomposes the min-cardinality problem into a master (attacker) problem (an integer program) and an operator subproblem (a mixed-integer program), and then solves these two problems in an iterative manner, until either an optimal min-cardinality attack is obtained or all the attack vectors are exhausted.

Min-cardinality disruption problem: Recall that in problem (Mm), the attacker's goal is to determine an optimal attack of size at most k (attack resource). On the other hand, in the min-cardinality problem, the attacker computes a disruption with as few attacked DN nodes as possible to induce a loss to the operator greater than a pre-specified threshold target post-contingency loss, denoted $\mathcal{L}_{\text{target}}$. These two problems are equivalent to each other in the following sense. The loss \mathcal{L}_{Mm} in (Mm) is non-decreasing in k (due to the inequality constraint $\sum_{i \in \mathcal{N}} d_i \leq k$). Therefore, if the parameter $\mathcal{L}_{\text{target}}$ is gradually increased then the minimum attack cardinality computed by min-cardinality problem will be non-decreasing in $\mathcal{L}_{\text{target}}$. Thus, for a fixed budget k , the smallest $\mathcal{L}_{\text{target}}$ value at which the minimum attack cardinality changes from k to $k + 1$ will be the optimal value of problem (Mm). By implementing a binary search on the parameter $\frac{100\mathcal{L}_{\text{target}}}{\mathcal{L}_{\text{max}}}$ between 0 – 100%, we can determine the smallest $\mathcal{L}_{\text{target}}$ at which the minimum attack cardinality changes from k to $k + 1$. Conversely, if we can solve (Mm), then by implementing a binary search on the parameter k between 0 and N , we can determine the minimum attack cardinality whose optimal loss exceeds $\mathcal{L}_{\text{target}}$.

It turns out that application of BD algorithm to the min-cardinality problem decomposes the min-cardinality problem into two single-level MIPs, namely the master (attacker) problem and the operator subproblem. The master problem only has the attack variables, integrality constraints, and the Benders cuts; and its objective function is bounded. If the BD algorithm were applied to budget- k -max-loss problem instead, the corresponding master problem will have variables d and u and (1)-(11) as constraints. Besides the computational advantage in solving the min-cardinality problem, the quantity $\frac{100\mathcal{L}_{\text{target}}}{\mathcal{L}_{\text{max}}}$ is relevant from the viewpoint of DN resilience. For example, if we want to evaluate whether or not a DN is 80% resilient to a k cardinality attack, we can set $\mathcal{L}_{\text{target}} = 0.2\mathcal{L}_{\text{max}}$, and then check if the optimal value of the min-cardinality problem is smaller than or equal k .

Now, we detail the approach to solve the min-

cardinality problem. For given load and DG connectivity vectors kc and kg , we define a **configuration** vector as $\kappa := (kc, kg)$. Given an attack vector d , let $\mathcal{K}_d := \{(kc, kg) \in \{0, 1\}^{\mathcal{N}} \times \{0, 1\}^{\mathcal{N}} \text{ such that (10) holds}\}$, i.e. \mathcal{K}_d denotes the set of all possible post-disruption configuration vectors that the operator can choose from. Then, for a fixed attack d and a fixed configuration vector $\kappa \in \mathcal{K}_d$, consider the following linear program:

$$\begin{aligned} \mathcal{P}(d, \kappa) := \min_{\beta \in \mathcal{B}} L(u, x) \\ \text{s.t. } u = (\beta, \kappa), x \in \mathcal{X}(u), \end{aligned} \quad (\text{D-LP}) \quad (11)$$

Note that (D-LP) may not have feasible solutions as the chosen configuration vector κ may violate (5) or (8) in the set of constraints $\mathcal{X}(u)$. In this case, the value of $\mathcal{P}(d, \kappa)$ is set to ∞ .

Suppose that, for a given DN \mathcal{G} , we are concerned with a TN-side disturbance Δv_0 and a target $\mathcal{L}_{\text{target}}$ post-contingency loss. We say that an attack-induced disruption $d \in \mathcal{D}$ *defeats* a configuration $\kappa \in \mathcal{K}_d$ if $\mathcal{P}(d, \kappa) \geq \mathcal{L}_{\text{target}}$, and is *successful* if it defeats *every* $\kappa \in \mathcal{K}_d$. The above definition is analogous to the definition of successful attack considered in [9]. We can now state the *Min-cardinality disruption* problem as follows:

$$\begin{aligned} \min_{d \in \mathcal{D}} \sum_{i \in \mathcal{N}} d_i \\ \text{s.t. } \mathcal{P}(d, \kappa) \geq \mathcal{L}_{\text{target}} \quad \forall \kappa \in \mathcal{K}_d. \end{aligned} \quad (\text{MCP})$$

If there exists an optimal solution of the problem (MCP), say d^* , then it is a *min-cardinality disruption* corresponding to $\mathcal{L}_{\text{target}}$ because it is successful and has minimum number of attacked nodes.

However, problem (MCP) is not tractable in its current form because the number of constraints are equal to the cardinality of set \mathcal{K}_d which can be exponential in $|\mathcal{N}|$, and verifying each constraint ($\mathcal{P}(d, \kappa) \geq \mathcal{L}_{\text{target}}$) is itself a linear optimization problem. Fortunately, the BD algorithm can be applied to address this issue.

Benders Decomposition: The algorithm decomposes (MCP) into two relatively simpler mixed-integer (MIP) subproblems: attacker subproblem (A-MIP) and operator subproblem (D-MIP). Both these problems are then solved in an iterative manner. In fact, in each iteration, one needs to solve (A-MIP), (D-MIP), and the dual of the problem in (D-LP), as discussed below. Fig. 4 summarizes the overall approach.

The attacker MIP can be written as follows:

$$\begin{aligned} \min_{d \in \mathcal{D}} \sum_{i \in \mathcal{N}} d_i \\ \text{s.t. } \text{set of Benders cuts,} \end{aligned} \quad (\text{A-MIP})$$

The master problem is initialized with only the integrality and budget constraints on the attack variables, and without any Benders cut. In each iteration, solving the master problem (A-MIP), which is a bounded MIP, if feasible, yields an attack d^* . Then, this attack vector is used as an input parameter for the operator subproblem (D-MIP).

For a fixed disruption d^* , the operator subproblem is the same as the inner problem of (Mm):

$$\begin{aligned} \min_{u \in \mathcal{U}(d^*)} \quad & L(u, x) \\ \text{s.t.} \quad & x \in \mathcal{X}(u), (11). \end{aligned} \quad (\text{D-MIP})$$

The problem (D-MIP) is also a bounded MIP because the load and DGs have bounded feasible space. If (D-MIP) is feasible, it yields an optimal operator response u^* and network state x^* for the disruption d^* . The operator's loss $L(u^*, x^*)$ will either exceed the target loss $\mathcal{L}_{\text{target}}$, in which case the algorithm terminates having successfully determined an optimal min-cardinality attack. Otherwise, $L(u^*, x^*) < \mathcal{L}_{\text{target}}$ which implies that d^* is not a successful disruption. In this case, we need to generate a Benders cut to eliminate d^* from the feasible space of (A-MIP).

To obtain a Benders cut, we select integer variables from the operator response $u^* = (\beta^*, \kappa^*)$; i.e. select the configuration vector κ^* . Note that problem (D-LP) with parameters (d^*, κ^*) can be simplified and rewritten as the following problem whose dual is written alongside:

$$\begin{array}{ll} \underbrace{\min_w c^T w}_{\text{Primal}} & \underbrace{\max_{\lambda \geq 0} (b + Bd^*)^T \lambda}_{\text{Dual}} \\ \text{s.t. } A_{eq} w = b_{eq} + B_{eq} d^* & \text{s.t. } A^T \lambda = c \\ & A_{in} w \geq b_{in} + B_{in} d^* \end{array} \quad (\text{D-LP1})$$

Here w and λ are the primal and dual decision vector variables; $A = [A_{eq}^T A_{in}^T]^T$, $B = [B_{eq}^T B_{in}^T]^T$ are matrices and $b = [b_{eq}^T b_{in}^T]^T$ is a vector of appropriate dimensions. We solve the dual problem (thanks to strong duality, the optimal values are the same) in (D-LP1) to compute $\mathcal{P}(d^*, \kappa^*)$ and an optimal dual solution λ^* . This furnishes a Benders cut, which is added to master problem in the next iteration. In particular, if the dual problem in (D-LP1) has an optimal solution λ^* , and its optimal value is L^* , then $\lambda^{*T} (b + Bd) \geq L^* + \epsilon$ is the desired Benders cut where ϵ is a small positive number. Note that d^* does not satisfy this Benders cut constraint because $\lambda^{*T} (b + Bd^*) = \mathcal{P}(d^*, \kappa^*) = L^* < L^* + \epsilon$, where the first equality holds because of strong duality in linear programs.

In each iteration, we eliminate suboptimal attack vectors from the feasible space of (A-MIP). Hence, the new master problem obtained by adding a Benders cut is a stronger relaxation of (MCP). Consequently, we get a progressively tighter lower bound on the minimum cardinality of the attack as the iteration continues, until we get a successful attack. Since there are finite number of attack vectors, whether successful or not, the BD algorithm is bound to terminate. As we will see in Sec. V-C, the BD algorithm takes significantly fewer number of iterations in comparison to a simple enumeration.

Computational issues: The choice of ϵ in the generation of Benders cut is an important issue in our implementation of BD algorithm. If we choose too large

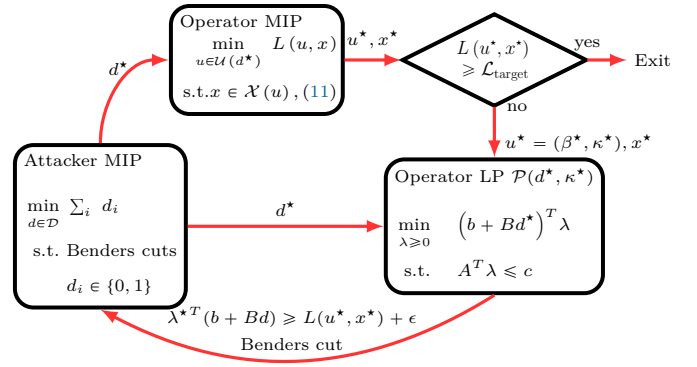


Fig. 4: Computational approach to solve (MCP)

an ϵ then many attack vectors (possibly including the optimal attack vectors) would be eliminated from the set of feasible attacker strategies in (A-MIP). If we choose too small an ϵ , then in each iteration only the current min-cardinality attack vector is eliminated resulting in a performance no better than simple enumeration over all attack vectors.

Another issue that we encountered is as follows. Recall that in problem (Mm), the coupling constraints (10) involve only the attack variables and operator integer variables. When we fix these attack variables and inner integer variables in (10), the resulting linear program (D-LP) has constraints of the form $0 \geq 0$, $1 \geq 0$ or $1 \geq 1$. The values of the optimal dual variables (λ^*) corresponding to these constraints (10) turn out to be 0, which are not useful in forming good Benders cuts. To address this issue, we modified the constraints to ensure that the coefficients of the attack variables (d) and the coefficients of inner continuous variables (pg, qg) are positive. One way to achieve this is to replace (4) and (10) by the following constraints:

$$kg_i \geq d_i, \quad (14a)$$

$$pg_i \leq (1 - d_i) \overline{pg}_i, \quad qg_i \leq (1 - d_i) \overline{qg}_i, \quad (14b)$$

$$pg_i \leq (1 - kg_i) \overline{pg}_i, \quad qg_i \leq (1 - kg_i) \overline{qg}_i, \quad (14c)$$

$$pg_i \geq (1 - kg_i) \overline{pg}_i, \quad qg_i \geq (1 - kg_i) \overline{qg}_i, \quad (14d)$$

Note that (4) and (10) are equivalent to (14). In addition, using the constraints (14a), (14b) and (4) does not render useful Benders cuts because the implementation solver assigns non-zero dual variables to the equality constraints (4) but not to (14b). Hence, (4) needs to be replaced by (14c)-(14d). Although for $(d_i, kg_i) = (1, 1)$, the constraints (14c) and (14d) are equivalent to (14b), the implementation solver assigns non-zero dual variables to the inequality constraints that come up earlier in the implementation. Hence, these two sets of inequality constraints are placed *after* (14b). With this replacement, the values of the optimal dual variables (λ^*) corresponding to the constraints (14b) will be non-zero, which ensures that useful Benders cuts ($\lambda^{*T} (b + Bd) \geq L^* + \epsilon$) will be generated in each iteration of the BD algorithm.

C. Computational Study

Now, we present computational results to show: (a) the value of timely operator response compared to no response; (b) comparison of the solutions of our BD approach with the optimal solution (generated for small networks by pure enumeration); and (c) the scalability of our approach to larger networks. We use three test networks for this purpose. We refer the reader to the appendix for the setup of our computational study.

Value of timely response: Recall that in Sec. I, we used post-contingency loss to define the resilience metric for operator response (\mathcal{R}_{Mm}) and no response (\mathcal{R}_{NR}) cases; and that $\mathcal{R}_{\text{Mm}} \geq \mathcal{R}_{\text{NR}}$. Fig. 5 compares the resiliency values for the two cases for varying number of nodes attacked, where computation of \mathcal{R}_{Mm} (resp. \mathcal{R}_{NR}) involves using BD algorithm (resp. Algorithm 1). Indeed, under no operator response, the voltage bound violations cause even the non-disrupted DGs to disconnect resulting in a cascade. However, under operator response, the substation automation detects these voltage bound violations, and preemptively exercises load control and/or disconnect the loads/DGs to reduce the total number of non-disrupted DGs from getting disconnected, and minimize the impact of attack. The difference between the two resiliency curves gives the value of timely response via the SA system. The intermediate curves in Fig. 5 correspond to the DN resilience under random attacks and no response by the operator. Finally, when both TN-side disturbance and DN attack are simultaneous, the resilience metric of DN decreases; see Fig. 5b.

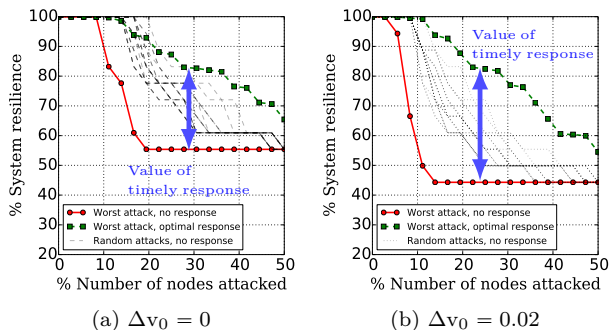


Fig. 5: Value of timely response ($N = 36$)

Benders Decomposition method vs. Simple enumeration: For a fixed cardinality k , we compute the optimal loss \mathcal{L}^* using simple enumeration over all disruptions. Then, we use \mathcal{L}^* as the parameter $\mathcal{L}_{\text{target}}$ for the problem (MCP). If the BD algorithm applied to (MCP) computes a successful attack with the same cardinality k , then indeed we have obtained the optimal attack of cardinality k . Fig. 6 shows that our method performs very well in computing optimal attacks. The inaccuracies result from the introduction of ϵ in the Benders cuts; see Sec. V-B.

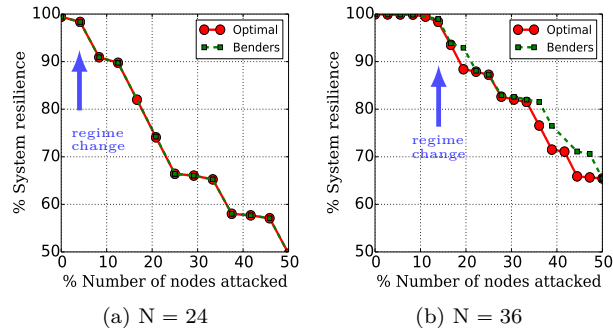


Fig. 6: Accuracy of BD algorithm in computing resilience metric in comparison to simple enumeration. Regime change from ND to CD is marked.

Scalability of BD algorithm: We tabulate the computational time required by the BD algorithm to compute min-cardinality attacks for different network sizes and varying values of the resilience metric $\mathcal{R}_{\text{target}} = 100(1 - \mathcal{L}_{\text{target}}/\mathcal{L}_{\text{max}})$; see Table II. Note that even for $N = 118$ nodes, which has 2^{118} configuration vectors, the BD algorithm finishes computations in ≈ 10 minutes. In comparison, for $N = 36$ node network, the simple enumeration method took ≈ 2 hours. The failure cases in Table II correspond to the cases when there does not exist an attack vector that exceeds the target loss values.

Entries are resilience metric of DN (in percentage), number of iterations (written in brackets), time (in seconds), attack cardinality.			
$\mathcal{R}_{\text{target}}$	$N = 24$	$N = 36$	$N = 118$
99	98.75, (3), 0.04, 1	98.96, (11), 0.22, 5	98.52, (27), 1.86, 14
95	91.15, (6), 0.08, 2	93.82, (13), 0.27, 6	94.66, (39), 3.34, 17
90	89.75, (10), 0.16, 3	88.08, (15), 0.34, 8	89.94, (50), 5.44, 26
85	82.41, (11), 0.18, 4	82.93, (17), 0.4, 10	84.96, (69), 9.23, 44
80	74.38, (14), 0.26, 5	76.99, (21), 0.52, 14	79.71, (86), 613.42, 52
75	74.38, (14), 0.26, 5	71.1, (23), 0.59, 16	
65	58.01, (20), 0.41, 9	Failure	Failure
55	49.65, (23), 0.47, 12		
45	Failure		

TABLE II: Resiliency metric evaluated using BD algorithm for 118 node network. The realized resilience metric can significantly fall short of the target resilience metric ($\mathcal{R}_{\text{target}} = 100(1 - \mathcal{L}_{\text{target}}/\mathcal{L}_{\text{max}})$); for example, when the attack cardinality changes from 1 to 2, the percentage resilience for 24-node network decreases sharply from 98.75% to 91.15% (which involves change from ND regime to CD regime). This means that the 24-node DN is at least 90% (actual value 91.15%) resilient to $k = 2$ cardinality attacks.

VI. CONCLUDING REMARKS

In this article, we developed an approach to evaluate a distribution system's resilience under a class of cyber and physical disruptions. We considered an attack model that involves a TN-side voltage disturbance, and DN-side supply-demand disturbance due to simultaneous DG disruptions. We also estimated the value of timely operator

response which involves preemptive load control or component disconnections implemented via the substation automation. In the companion paper [23], we refine our model of attacker-operator interaction. First, we extend the operator model to include (a) microgrid islanding capabilities to form subnetworks that can operate without being connected to the main grid, and (b) dispatch of controllable distributed energy resources (DERs). We also introduce a trilevel formulation in which the operator uses controllable DERs as contingency reserves before the disruption. These reserves can be dispatched to limit the impact of contingencies resulting from cyber-physical failure events. Finally, we investigate how the system performance can recover by reconnection of the disrupted DGs and loads, and changing the mode of microgrid operations from islanding to grid-connected mode.

REFERENCES

- [1] M. Farivar and S. H. Low, "Branch flow model: Relaxations and convexification - part i," *IEEE Transactions on Power Systems*, vol. 28, no. 3, pp. 2554–2564, 2013.
- [2] N. C. Scott, D. J. Atkinson, and J. E. Morrell, "Use of load control to regulate voltage on distribution networks with embedded generation," *IEEE Transactions on Power Systems*, vol. 17, no. 2, pp. 510–515, 2002.
- [3] K. Turitsyn, P. Sulc, S. Backhaus, and M. Chertkov, "Options for control of reactive power by distributed photovoltaic generators," *Proceedings of the IEEE*, vol. 99, no. 6, pp. 1063–1073, 2011.
- [4] D. Shelar, S. Amin, and I. Hiskens, "Towards resilience-aware resource allocation and dispatch in electricity distribution networks," *Book chapter in Springer/IMA volume on the control of energy markets and grids*, 2018.
- [5] A. Lee, "Electric sector failure scenarios and impact analyses," National Electric Sector Cybersecurity Organization Resource (NESCOR), Electric Power Research Institute (EPRI), Palo Alto, California, Tech. Rep.
- [6] J. Liang, L. Sankar, and O. Kosut, "Vulnerability analysis and consequences of false data injection attack on power system state estimation," *IEEE Transactions on Power Systems*, vol. 31, no. 5, pp. 3864–3872, 2016.
- [7] F. Pasqualetti, F. Dörfler, and F. Bullo, "Attack detection and identification in cyber-physical systems," *IEEE Transactions on Automatic Control*, vol. 58, no. 11, pp. 2715–2729, 2013.
- [8] D. Shelar and S. Amin, "Security assessment of electricity distribution networks under DER node compromises," *IEEE Transactions on Control of Network Systems*, vol. 4, no. 1, pp. 23–36, 2017.
- [9] D. Bienstock and A. Verma, "The N-k problem in power grids: New models, formulations, and numerical experiments," *SIAM J. on Optimization*, vol. 20, no. 5.
- [10] J. Salmeron, K. Wood, and R. Baldick, "Worst-case interdiction analysis of large-scale electric power grids," *IEEE Transactions on Power Systems*, vol. 24, no. 1, pp. 96–104, 2009.
- [11] K. C. Sou, H. Sandberg, and K. Johansson, "Computing critical k-tuples in power networks," *Power Systems, IEEE Transactions on*, vol. 27, no. 3, pp. 1511–1520, 2012.
- [12] N. I. A. Council, "Critical infrastructure resilience final report and recommendations," 2009.
- [13] J. Zhao, C. Wang, B. Zhao, F. Lin, Q. Zhou, and Y. Wang, "A review of active management for distribution networks: Current status and future development trends," *Electric Power Components and Systems*, vol. 42, no. 3-4, pp. 280–293, 2014.
- [14] N. R. Standards, "CIP-005-5 – Cyber Security - Electronic Security Perimeter(s)," 2015.
- [15] R. Lee, M. Assante, and T. Conway, "Analysis of the cyber attack on the Ukrainian power grid, electricity information sharing and analysis center," 2015.
- [16] R. Wood, "Bilevel network interdiction models: Formulations and solutions," in *Wiley Encyclopedia of Operations Research and Management Science*, 2011.
- [17] L. Zhao and B. Zeng, "Vulnerability analysis of power grids with line switching," *IEEE Transactions on Power Systems*, vol. 28, no. 3, pp. 2727–2736, 2013.
- [18] M. Baran and F. F. Wu, "Optimal sizing of capacitors placed on a radial distribution system," *IEEE Transactions on Power Delivery*, vol. 4, no. 1, pp. 735–743, 1989.
- [19] "IEEE Standard for Interconnection and Interoperability of Distributed Energy Resources with Associated Electric Power Systems Interfaces," *IEEE Std 1547-2018 (Revision of IEEE Std 1547-2003)*, pp. 1–138, 2018.
- [20] S. Fuloria, R. Anderson, K. Mcgrath, K. Hansen, and O. Alvarez, "The protection of substation communications," 2012.
- [21] "Power Quality – Voltage Disturbances (Chapter 25)," in *Transmission and Distribution Electrical Engineering (Third Edition)*, C. Bayliss and B. Hardy, Eds. Newnes.
- [22] N. S. M. S. (SMS), "Fault Induced Delayed Voltage Recovery (FIDVR) Advisory," July 2015. [Online]. Available: <https://goo.gl/Xy6Vwv>
- [23] D. Shelar, S. Amin, and I. Hiskens, "Resilience of Electricity Distribution Networks - Part II: Resource Allocation and Dispatch."
- [24] D. Bienstock, *Electrical transmission system cascades and vulnerability - an operations research viewpoint*, ser. MOS-SIAM Series on Optimization. SIAM, 2016, vol. 22.
- [25] A. Teixeira, H. Sandberg, and K. H. Johansson, "Networked control systems under cyber attacks with applications to power networks," in *Proceedings*

- of the 2010 American Control Conference, 2010, pp. 3690–3696.
- [26] Y. Liu, P. Ning, and M. K. Reiter, “False data injection attacks against state estimation in electric power grids,” *ACM Trans. Inf. Syst. Secur.*, vol. 14, no. 1.
- [27] D. Shelar, P. Sun, S. Amin, and S. Zonouz, “Compromising Security of Economic Dispatch in Power System Operations,” in *47th Annual IEEE/IFIP International Conference on Dependable Systems and Networks (DSN)*, 2017.
- [28] Y. P. Agalgaonkar, B. C. Pal, and R. A. Jabr, “Distribution Voltage Control Considering the Impact of PV Generation on Tap Changers and Autonomous Regulators,” *IEEE Transactions on Power Systems*, vol. 29, no. 1, pp. 182–192, 2014.

APPENDIX

Related Work: Several papers have used bilevel optimization formulations for vulnerability assessment of TNs to adversarial disruptions [7, 9, 10, 11]. Another notable application is the generalization of the classical N-1 security problem to an N-k problem [9, 11]. These formulations typically assume the DC power flow approximation, which enables a solution approach based on KKT-based reformulation, and leads to single-level Mixed-Integer Program (MIP). In our past work, we used a similar formulation to assess the security of DNs to remotely induced DG disruptions [4, 8]. However, that formulation did not consider preemptive tripping of loads/DGs as a part of the operator’s response strategy, and thus it does not require the inner problem of the bilevel program to have integer variables. A simple greedy heuristic gave reasonable performance in that case. In contrast, in this paper, we deal with a bilevel program with mixed-integer variables in the inner problem.

Modeling of cyberattacks on node dynamics in electricity networks as nodal disturbances has been studied previously [25]. However, their model assumes that the components remain connected to the network after the attack. Perhaps the most extensively studied security attack model for power systems is the false data injection attack, in which the attacker aims to compromise the integrity of state estimation algorithms; see for example [6, 26, 27]. Biased estimates of network state resulting from such an attack can negatively impact the contingency planning and other crucial operator decisions. Most papers focusing on this model do not focus on analyzing the impact of incorrect operator decisions, although recent work has considered how such integrity attacks can lead to inefficient economic dispatch solutions, or cause in operating bound violations resulting in unsafe state [6, 27]. A distinctive feature of our formulation is that we consider tripping of DN components, which can either result from operating bound violations induced by cyber-physical failure events, or from response of the operator who decides to preemptively trip certain components

to prevent progressive disconnects of larger number of components.

Justification of the security attack model: Our attack model is motivated by the security failure scenarios listed in [5]. These scenarios capture the capabilities of the following threat actors: (a) cyber-hackers of an enemy nation motivated to disrupt supply to critical facilities, (b) a malicious adversary looking to extort ransom money from the utility, or (c) a disgruntled internal employee motivated by revenge. The Ukraine attack is an example of type (a). The DN cyber architecture can have existing vulnerabilities such as non-confidentiality of control commands, lack of multi-factor authentication, incorrect firewall rules that allow unauthorized access, etc. A threat actor could exploit these vulnerabilities to launch replay attacks, or a server-side attack at the control center, or hack operator credentials, any of which could allow him to do malicious activities such as mass remote disconnect of components. In this paper, we model the DN-side disruptions as nodal supply-demand disturbances. For example, mass disconnects of DGs (resp. loads) can cause loss of supply (resp. demand). Additionally, a threat actor could program his attack to be launched simultaneously with a TN-side disruption. The overall framework for modeling impact of cyber-physical disruptions to DN is illustrated in Fig. 7.

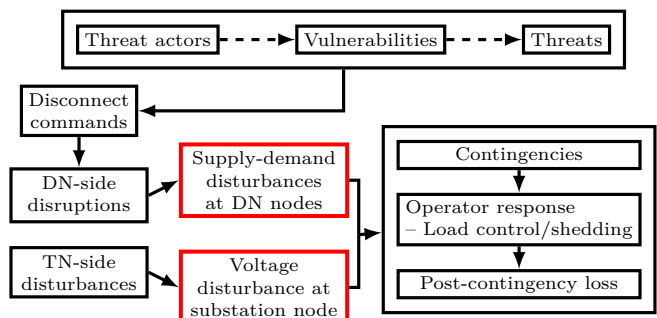


Fig. 7: Framework for modeling impact of cyber-physical failures on DNs.

Remark on traditional response mechanisms to voltage regulation: In addition to response via SA system that we consider in this paper, other types of classical actions implemented through control of voltage regulators and capacitors as well as network reconfiguration can also form part of the operator response. However, we chose load control and intentional disconnects due to the following reasons: first, the time-scale of disturbance created by the attack can be very small (few seconds), and can trigger an immediate cascade of component disconnects due to operating bound violations. Typically, voltage regulators and capacitor banks require a larger response time; in fact, frequent activation of these devices is not preferred as they are subject to mechanical wear and tear [28]. On the other hand, thanks to advancements in substation automation and power electronics

based control of loads/DGs, our response strategy can be implemented within a few milliseconds after the diagnostic information about the timing of attack-induced disruption and extent of TN-side disturbance is obtained. However, our modeling framework can be extended to situations where appropriate changes in the settings of voltage regulators and capacitor banks are deemed as desirable aspects of operator response. These can be incorporated as integer decision variables in the inner problem of the bilevel formulation.

Remarks about Algorithm 1: Note that Algorithm 1 prioritizes DG disconnects over load disconnects for the purpose of limiting voltage bound violations. We justify this as follows. Typically, the operating bounds for DGs are more restrictive than for the loads, as the voltage drop at a DG node can be an indicator of fault during which the supply from DG should be interrupted. Specifically, according to the rules for interconnection of DGs, if the nodal voltage is below 0.8 pu or above 1.2 pu, then the corresponding DG should trip within 2 seconds [19]. On the other hand, the loads can tolerate voltage bound violations for about few minutes. The response times of the voltage regulators along the feeders and online-load-tap-changing (OLTC) transformer at the substation are about 15 and 30 seconds, respectively. Furthermore, if along a feeder, there are more than one of these devices, then the total response time is a sum of the response times of the individual devices. Hence, with a OLTC transformer and 3 voltage regulators along a feeder, the total response time can be about 75 seconds, which is acceptable only because the loads can tolerate voltage bound violations for a few minutes.

Comments about cost coefficients:

- 1) The typical values for the parameters in Eq. (12) of the cost terms are listed in Table III.

Weights	Typical values
W_{LC}	$\frac{1}{4} \times 11$ cents per kilowatt hour
W_{VR}	$\frac{2}{100} \times 11$ cents per kilowatt hour
W_{LS}	3 dollars per kilowatt hour

TABLE III: Typical values of cost parameters.

- 2) The weight $W_{LS} - W_{LC}$ is chosen to enable proper counting of the cost of load control when the load is disconnected. Also, we have included the cost of load shedding, but not the cost of disconnection of customer-owned DGs because it's conceivable that the customers will be significantly more inconvenienced if there is load shedding as opposed to DG disconnections during a contingency. However, we can easily account for the cost of DG disconnections in our formulation.

Setup for computational study: We consider three networks: 24 node, and modified IEEE 36 node and 118 node network. Each line has an identical impedance of

$r_{ij} = 0.01$, $x_{ij} = 0.02$. 50 % of the nodes have a DG each and 50% have a load each. Consider a parameter $\alpha = \frac{6}{N}$. Before the contingency, each DG has active power output of $\overline{p\mathbf{g}}_i = \alpha$, and each load has a demand of $\overline{p\mathbf{c}}_i = 1.25\alpha$. Thus, we assume 80% DG penetration since the total DG output is 80% of the total demand. The voltage bounds are $\underline{v\mathbf{c}}_i = 0.9$, $\overline{v\mathbf{c}}_i = 1.1$, $\underline{v\mathbf{g}}_i = 0.92$ and $\overline{v\mathbf{g}}_i = 1.08$. The reactive power values are chosen to be exactly one third that of the corresponding active power value, i.e. a 95% power factor value for each load and DG. The values are chosen such that the total net active power demand in the DN is 0.75 pu, and the lowest voltage in the network before any contingency is close to $\underline{v\mathbf{g}}$. The maximum load control parameter is $\underline{\beta}_i = 0.8$, i.e. at most 20% of each load demand can be curtailed. For the sake of simplicity, we assume that all DGs and loads are homogeneous. $W_{LC} = \frac{100}{\overline{p\mathbf{c}}_i}$, $W_{VR} = 100$, $W_{LS} = \frac{1000}{\overline{p\mathbf{c}}_i}$.

All experiments were performed on a 2.8 GHz Intel Core i7 with 16 GB 1600 MHz DDR3 MacBook Pro laptop.

Description of Fig. 2: The figure shows how system performance evolves over time after the attacker-operator interaction. Initially, the DN is operating in nominal conditions. As a result of the disturbances (from the TN- and/or DN-side), the system performance degrades. If the operator fails to respond in a timely manner, then an uncontrolled cascade can occur due to automatic disconnections of components. This would result in a post-contingency loss \mathcal{L}_{NR} . Eventually, the operator undertakes secondary control actions like changing tap settings of transformers, or switching on capacitor banks. Thus, the nodal voltages recover, allowing the disconnected loads to be reconnected, and operate within safe operating bounds. Thus, the DN gradually returns to its nominal operation.

However, during the time the DN's performance is degraded, the operator can respond by exercising load control and/or preemptive disconnection of components. This response can be used to avoid an uncontrolled cascade, and limit the post-contingency loss to \mathcal{L}_{Mm} . The operator can now reconnect the disrupted DGs. This allows the nodal voltages to recover, thereby allowing reconnections of disconnected loads. Thus, the operator is able to restore the system performance sooner than the case of no response, possibly without resorting to the classical secondary control actions.

The lower post-contingency loss and quicker recovery together constitutes a DN's resilience to attacker-induced events. In the companion paper, we address other aspects of DN resilience. Specifically, we consider the strategic resource allocation to further minimize the post-contingency loss, as well as reconnections of disrupted DGs to enable faster DN recovery.

Example for problem (D-LP1): Recall the primal problem in (D-LP1). With the help of an example, we show how to instantiate the primal problem. Consider a

DN \mathcal{G} with nodes $\{0, 1\}$ and line $(0, 1)$. Then the variable w is given as:

$$w = (\beta_1, pg_1, qg_1, p_1, q_1, P_1, Q_1, v_0, v_1, t),$$

where t is an auxiliary variable. The corresponding cost vector c is given as:

$$c = (-W_{LC}, 0, 0, 0, 0, W_{AC}, 0, 0, 0, 0, W_{VR}). \quad (15)$$

Furthermore, we are given the parameters d and $\kappa = (kc_1, kg_1)$. Then, the constraints of the problem (D-LP1) are given as follows:

$$w \geq \begin{array}{c} \overbrace{\begin{bmatrix} 0 & 1 & 0 & 0 & 0 & 0 & 0 & 0 & 0 & 0 \\ 0 & -1 & 0 & 0 & 0 & 0 & 0 & 0 & 0 & 0 \\ 0 & 0 & 1 & 0 & 0 & 0 & 0 & 0 & 0 & 0 \\ 0 & 0 & -1 & 0 & 0 & 0 & 0 & 0 & 0 & 0 \\ 0 & 1 & 0 & 0 & 0 & 0 & 0 & 0 & 0 & 0 \\ 0 & -1 & 0 & 0 & 0 & 0 & 0 & 0 & 0 & 0 \\ 0 & 0 & 1 & 0 & 0 & 0 & 0 & 0 & 0 & 0 \\ 0 & 0 & -1 & 0 & 0 & 0 & 0 & 0 & 0 & 0 \\ 0 & 0 & 0 & 0 & 0 & 0 & 0 & 0 & 1 & 0 \\ 0 & 0 & 0 & 0 & 0 & 0 & 0 & 0 & 0 & -1 \\ 0 & 0 & 0 & 0 & 0 & 0 & 0 & 0 & 1 & 0 \\ 0 & 0 & 0 & 0 & 0 & 0 & 0 & 0 & -1 & 0 \\ 1 & 0 & 0 & 0 & 0 & 0 & 0 & 0 & 0 & 0 \\ -1 & 0 & 0 & 0 & 0 & 0 & 0 & 0 & 0 & 0 \\ 0 & 0 & 0 & 0 & 0 & 0 & 0 & 1 & 1 & 0 \\ 0 & 0 & 0 & 0 & 0 & 0 & 0 & 0 & -1 & 1 \\ 0 & 0 & 0 & 0 & 0 & 0 & 0 & 0 & 0 & 1 \end{bmatrix}}^{A_{in}} \\ \end{array} + \begin{array}{c} \overbrace{\begin{bmatrix} \overline{p\mathcal{G}}_1 \\ -\overline{p\mathcal{G}}_1 \\ \overline{q\mathcal{G}}_1 \\ -\overline{q\mathcal{G}}_1 \\ (1-kg_1)\overline{p\mathcal{G}}_1 \\ -(1-kg_1)\overline{p\mathcal{G}}_1 \\ (1-kg_1)\overline{q\mathcal{G}}_1 \\ -(1-kg_1)\overline{q\mathcal{G}}_1 \\ \underline{v\mathcal{G}}_1 - kg_1 \\ -\overline{v\mathcal{G}}_1 + kg_1 \\ \underline{v\mathcal{C}}_1 - kg_1 \\ -\overline{v\mathcal{C}}_1 + kg_1 \\ (1-kc_1)\underline{\beta}_1 \\ -(1-kc_1)\overline{\beta}_1 \\ \underline{v}^{\text{nom}} \\ -\overline{v}^{\text{nom}} \\ 0 \end{bmatrix}}^{b_{in}} \\ \end{array} + \begin{array}{c} \overbrace{\begin{bmatrix} -\overline{p\mathcal{G}}_1 \\ \overline{p\mathcal{G}}_1 \\ -\overline{q\mathcal{G}}_1 \\ \overline{q\mathcal{G}}_1 \\ 0 \\ 0 \\ 0 \\ 0 \\ 0 \\ 0 \\ 0 \\ 0 \\ 0 \\ 0 \\ 0 \\ 0 \\ 0 \\ 0 \\ 0 \end{bmatrix}}^{B_{in}} \\ \end{array} d$$

$$w = \begin{array}{c} \overbrace{\begin{bmatrix} 0 & 0 & 0 & -1 & 0 & 1 & 0 & 0 & 0 & 0 \\ 0 & 0 & 0 & 0 & -1 & 0 & 1 & 0 & 0 & 0 \\ 0 & 0 & 0 & 0 & 0 & 2r_{01} & 2x_{01} & -1 & 1 & 0 \\ -\overline{p\mathcal{E}}_1 & 1 & 0 & 1 & 0 & 0 & 0 & 0 & 0 & 0 \\ -\overline{q\mathcal{E}}_1 & 0 & 1 & 0 & 0 & 0 & 0 & 0 & 0 & 0 \\ 0 & 0 & 0 & 0 & 0 & 0 & 0 & 0 & 0 & 1 \end{bmatrix}}^{A_{eq}} \\ \end{array} + \begin{array}{c} \overbrace{\begin{bmatrix} 0 \\ 0 \\ 0 \\ 0 \\ 0 \\ 0 \end{bmatrix}}^{b_{eq}} \\ \end{array} + \begin{array}{c} \overbrace{\begin{bmatrix} 0 \\ 0 \\ 0 \\ 0 \\ 0 \\ 0 \end{bmatrix}}^{B_{eq}} \\ \end{array} d$$

Finally, $A = \begin{bmatrix} A_{in} \\ A_{eq} \end{bmatrix}$, $B = \begin{bmatrix} B_{in} \\ B_{eq} \end{bmatrix}$, and $b = \begin{bmatrix} b_{in} \\ b_{eq} \end{bmatrix}$.